Supporting Information

Centimeter-Sized Single-Orientation Monolayer Hexagonal Boron Nitride With or Without Nanovoids

Huanyao Cun,*[,†,‡] Adrian Hemmi,[†] Elisa Miniussi,[†] Carlo Bernard,[†] Benjamin Probst,[¶] Ke Liu,[‡] Duncan T. L. Alexander,[§] Armin Kleibert,[∥] Gerson Mette,[†,□] Michael Weinl,[#] Matthias Schreck,[#] Jürg Osterwalder,[†] Aleksandra Radenovic,[‡] and Thomas Greber[†]

[†]*Physik-Institut and* [¶]*Department of Chemistry, Universität Zürich, 8057 Zürich, Switzerland*

[‡]*Institute of Bioengineering and* [§]*Centre Interdisciplinaire de Microscopie Électronique EPFL, 1015 Lausanne, Switzerland*

[∥]*IISwiss Light Source, Paul Scherrer Institut, 5232 Villigen, Switzerland*

[□]*Fachbereich Physik, Philipps-Universität Marburg, 35037 Marburg, Germany*

[#]*Institut für Physik, Universität Augsburg, 86159 Augsburg, Germany*

E-mail: huanyao.cun@epfl.ch

Table of Contents

1. Transfer of *h*-BN flakes with ”bubbling-only” method

Four different characterization methods are applied for the same transferred BN flakes on 80 nm SiO_2 with ”bubbling-only, no TOA-assist” approach by SEM, X-PEEM, optical microscopy and sample averaging XPS, as shown in Figure S1. The BN flakes marked with blue and red circles are the same in all images recorded in 3 different microscopes.

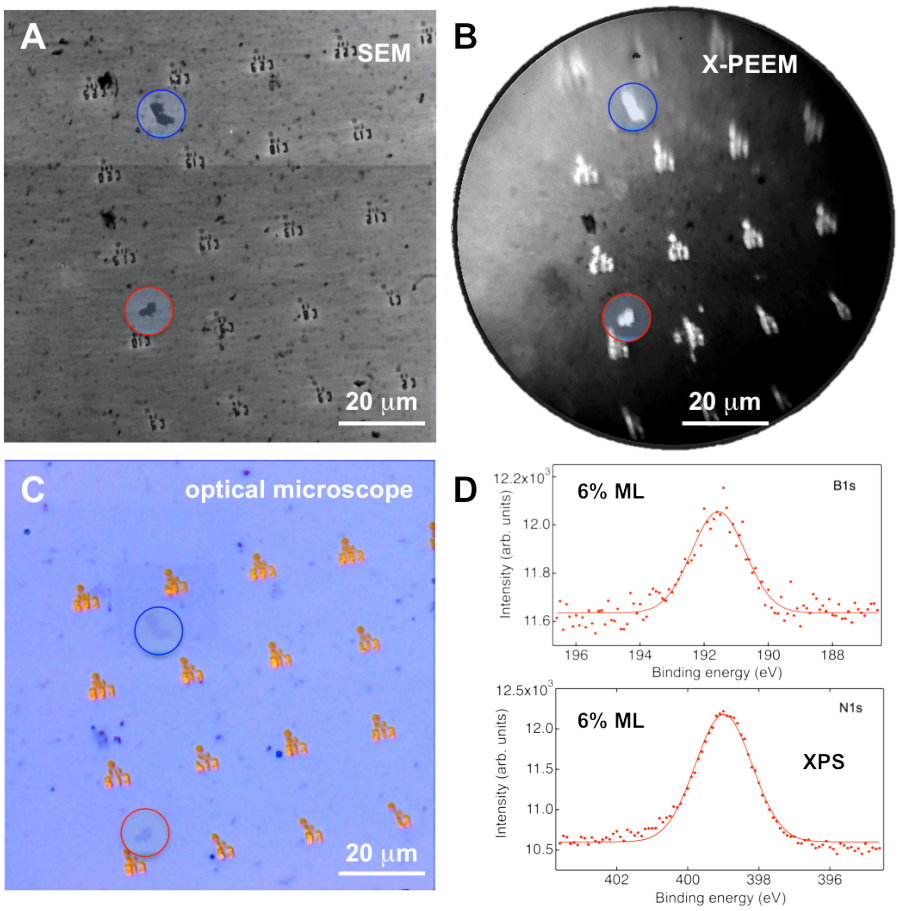

Figure S1: **Characterization of micrometer-sized *h*-BN flakes on 80 nm SiO_2 exfoliated from *h*- BN/Rh(111) without TOA^+-treatment.** The circles with the same colors (blue or red) in (A), (B) and (C) indicate the same individual flakes, as identified by gold markers on the SiO_2 substrate. (A) SEM. (B) X-PEEM image recorded at the boron K-edge (data taken at the SIM beamline of the Swiss Light Source). (C) Optical microscopy. (D) XPS B1s and N1s peaks of the same transferred BN sample on SiO_2.

2. Regrowth of *h*-BN on recycled Rh(111)

Rh(111) substrates after *h*-BN transfer were characterized by LEED (Figure S2B), XPS (Figure S2D and S2E) and atomic force microscopy (AFM) (Figure S2F). After *h*-BN delamination, the Rh(111) film was transferred back to UHV for characterization and a new preparation of *h*-BN monolayer by high-temperature CVD with borazine $(HBNH)_3$ as precursor.[1,2] The quality of second growth *h*-BN is as good as the preceding preparation as can be judged from LEED (Figure S2A and S2C and XPS (Figure S2D and S2E) .

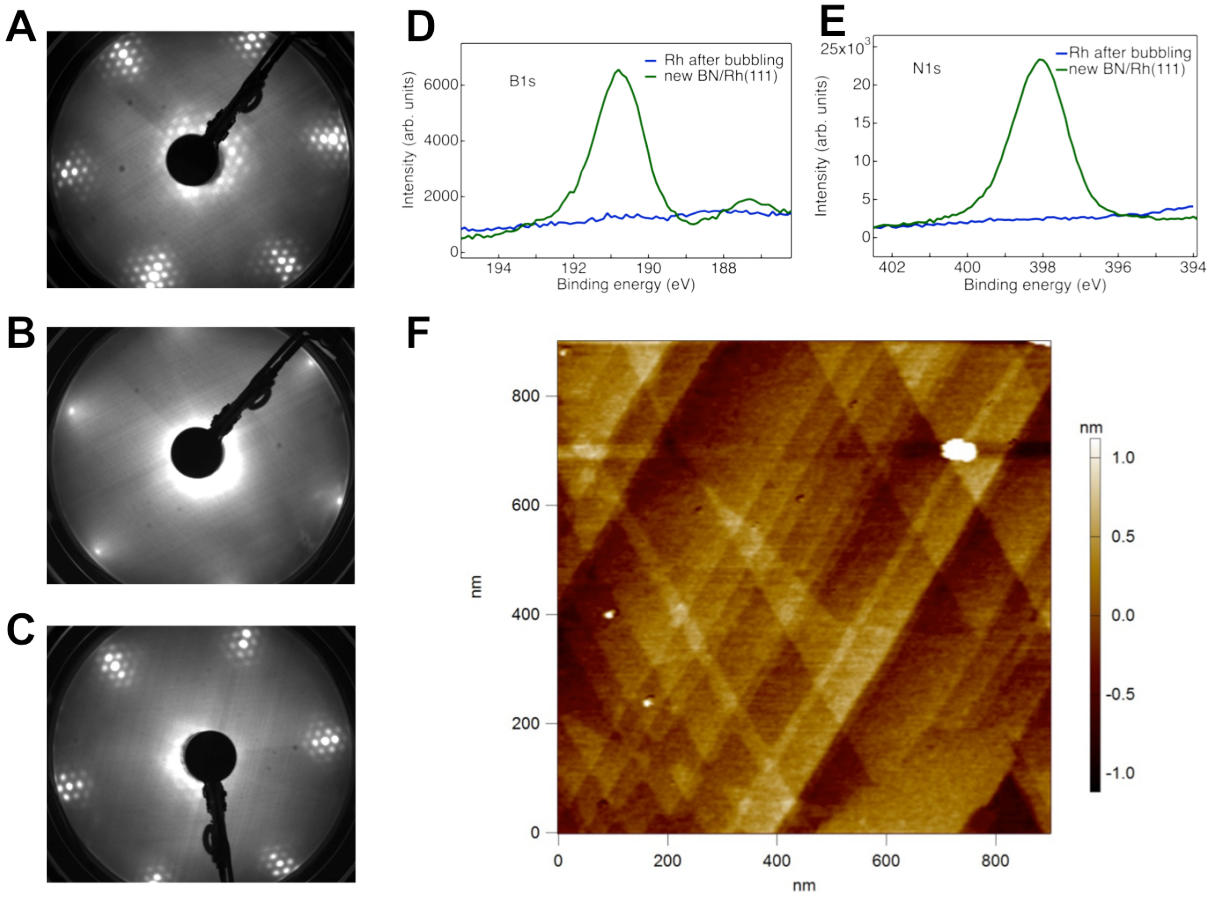

Figure S2: **Regrowth of *h*-BN nanomesh on used Rh(111) substrates.** (A-C) LEED patterns. (A) Pristine *h*-BN with the 13×13 BN on 12×12 Rh superstructure spots. (B) Rh(111) substrate after "bubbling" transfer. (C) Second growth of *h*-BN/Rh(111). XPS B1s (D) and N1s (E) peaks on the Rh film after transfer (blue) and regrown *h*-BN/Rh (green). (F) 900×900 nm^2 AFM image at room temperature shows the clean surface of a Rh(111) substrate after the *h*-BN transfer.

3. Survey spectra of *h*-BN monolayer before and after transfer

The XPS survey spectra of *h*-BN monolayer sample in Figure 3 of the main text were measured before (*h*-BN/Rh(111)) and after (*h*-BN/SiO_2) the transfer, as displayed in Figure S3.

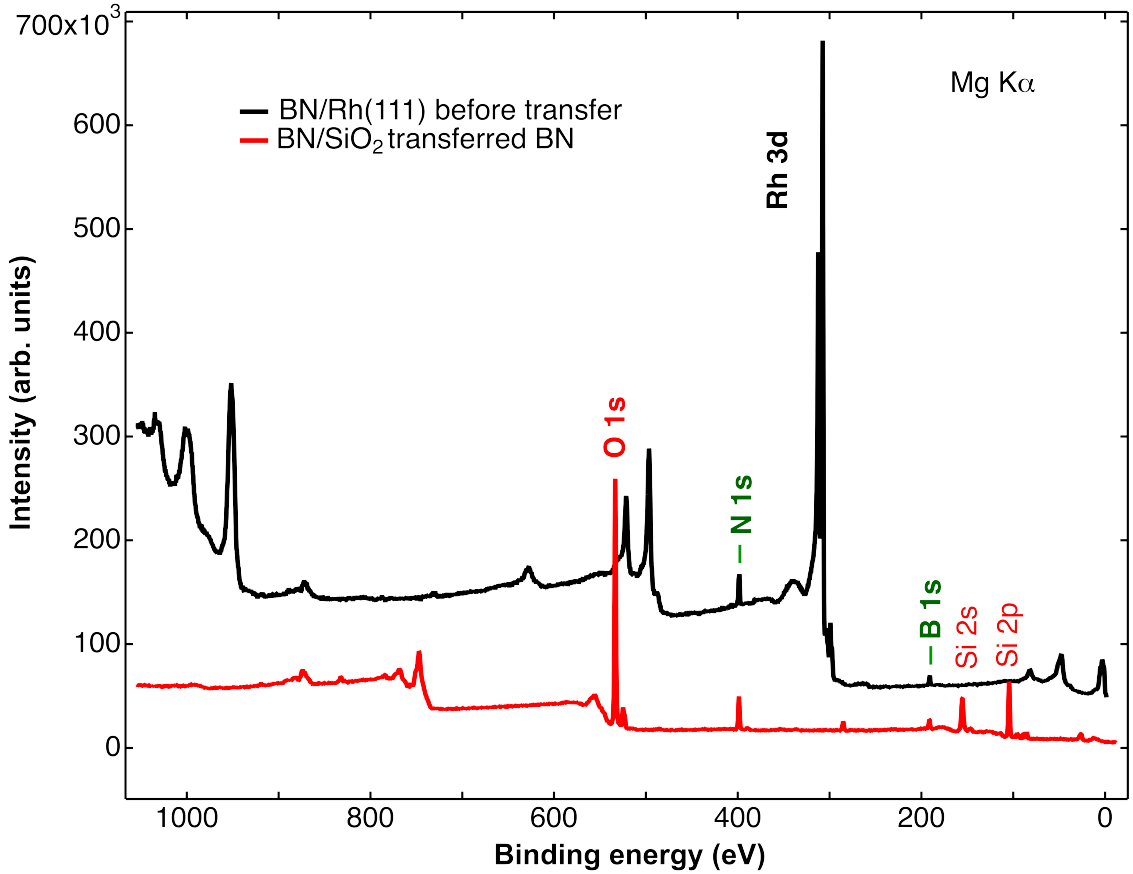

Figure S3: **Survey spectra of *h*-BN monolayer before and after transfer.** Mg Kα XPS ($\bar{h}\omega$ = 1253.6 eV) survey spectra with the same source and analyzer settings show the difference between before (black, *h*-BN/Rh(111)) and after (red, *h*-BN/SiO_2) membrane transfer. The transfer rate is above 95%, which is confirmed by the B1s and N1s peaks of *h*-BN/SiO_2 after transfer.

4. Determination of the transfer rate of *h*-BN monolayer

In order to determine the transfer rate of *h*-BN, three sets of XPS (MgKα, $\bar{h}\omega$ = 1253.6 eV) measurements are carried out for pristine *h*-BN/Rh(111), transferred *h*-BN/SiO_2, and used Rh(111) substrates after *h*-BN delamination, respectively. The three samples are typically annealed to 950 K (for *h*-BN/Rh(111) and used Rh(111) substrates) and 650 K for transferred *h*-BN/SiO_2. The B1s and N1s peaks of these three samples (derived from the same *h*-BN/Rh preparation) are integrated individually (I_{tot}, I_{tra} and I_{rem}). The peaks are measured with the same pass energy, sweep numbers and scan time. The peak integrals of the core levels of B1s (I_{totB}) and N1s (I_{totN}) are 100% for a

pristine *h*-BN monolayer. The B1s and N1s peak intensity ratios of transferred *h*-BN/SiO_2 (I_{traB} and I_{traN}) and pristine *h*-BN/Rh(111) are defined as the transfer rate σ_{tra}:

$$\sigma_{tra} = \frac{I_{traB(N)}}{I_{totB(N)}}$$

The remaining BN ratio (σ_{rem}) on the bubbled Rh(111) is defined as:

$$\sigma_{rem} = \frac{I_{remB(N)}}{I_{totB(N)}}$$

Therefore the lost BN ratio can be calculated as:

$$\sigma_{los} = 1 - \sigma_{tra} - \sigma_{rem}$$

Thus the removed BN ratio $\sigma_{remove} = \sigma_{tra} + \sigma_{los}$. Without loss, the transferred BN ratio σ_{tra} is the same as the removed BN ratio σ_{remove}. The correlation between transferred BN vs. removed BN based on 57 experiments is displayed in Figure S4. The light blue data points correspond to transfers without TOA^+-treatment, while dark blue and red colors are the experiments with TOA^+-treatment. Clearly, the electrochemical "bubbling" method without TOA^+-assist does not lead to complete *h*-BN monolayer transfer. The upper-right corner with $\sigma_{tra}/\sigma_{remove}$ = 1:1 is the ultimate goal for the transfer.

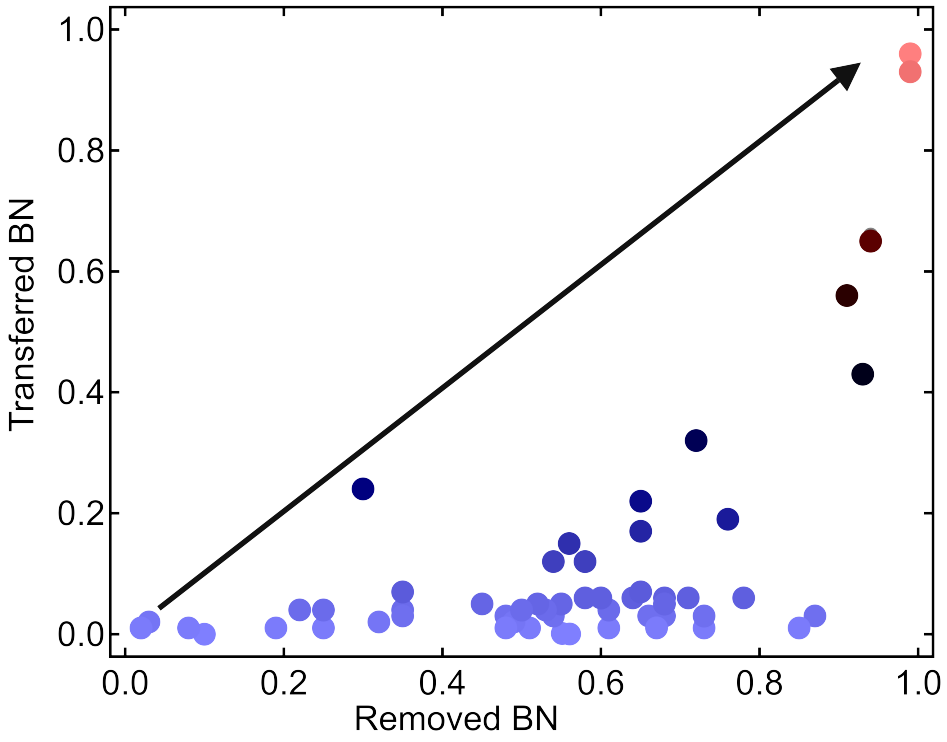

Figure S4: **Transfer rates vs. remove rates for different *h*-BN transfer samples.** The Y axis represents the transferred BN and X axis stands for the removed BN. The light blue color represents the transfers without TOA^+-assisted "bubbling", while transfer rates above 60% have only been obtained by TOA^+-assisted transfer. The black arrow indicates the maximum transfer at a given removal and the arrowhead points to the goal of "complete transfer".

5. Optical microscopy of continuous *h*-BN monolayer with TOA^+-assisted process

The continuous *h*-BN monolayers transferred on 80 nm SiO_2 can be observed with optical microscopy at room temperature after removal of PMMA, as shown in Figure S5. The size of transferred BN monolayer is 9.5×9.5 mm^2.

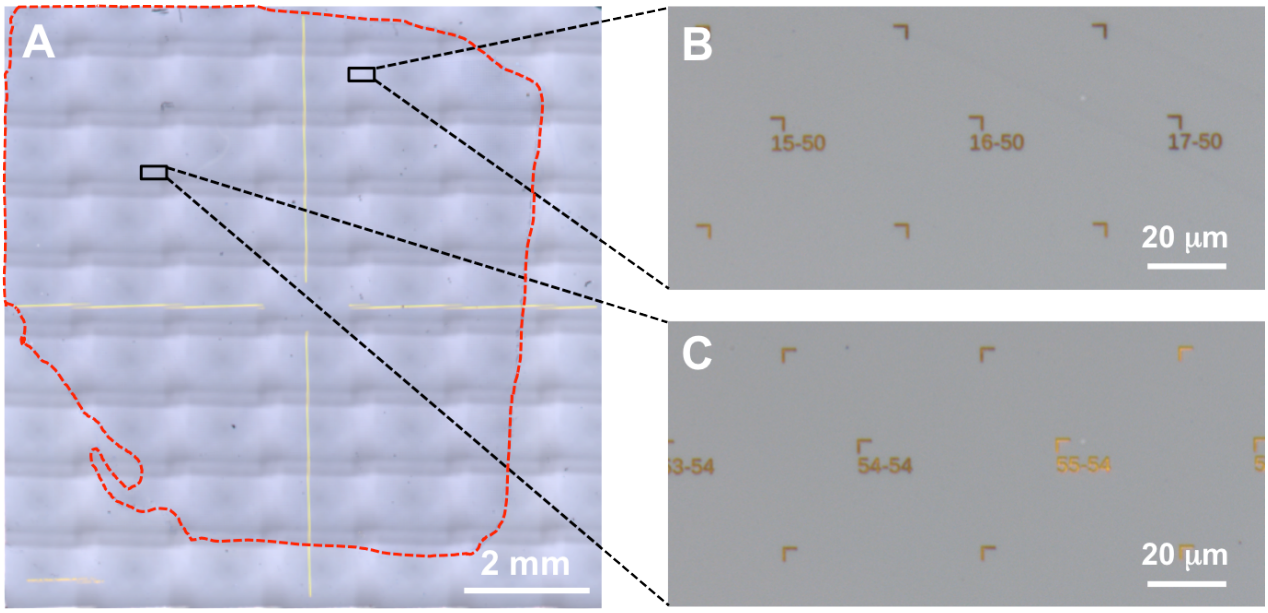

Figure S5: **Optical microscopy images of transferred *h*-BN/SiO2/Si.** (A) Optical microscopy overview image shows the entire transferred continuous *h*-BN monolayer with centimeter-size. The image was obtained by stitching multiple optical images with 150× magnification. The slightly darker region is the *h*-BN-covered area, which is marked with dashed red lines to guide the eyes (square shape with a cut-edge at left-bottom). (B) and (C) are two zoom-in images with 2000× magnification. The gold markers on SiO_2 are used for localizing specific spots on the surface in different instruments.

6. Raman spectrum

Raman spectra were measured with beam wavelengths of 455 nm. The fingerprint peak of *h*-BN at 1368 cm^{-1} is clearly identified[3] with an average full width at half maximum (FWHM) of 20 cm^{-1}.

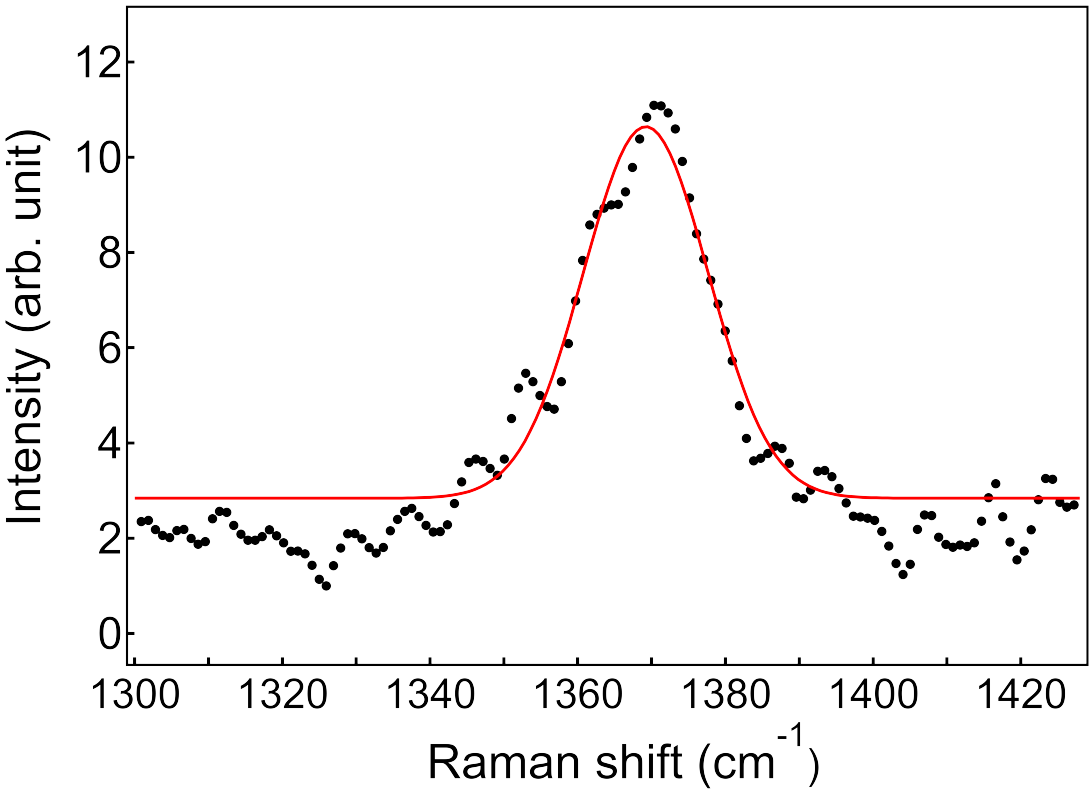

Figure S6: **Representative Raman spectrum of transferred *h*-BN/SiO_2/Si sample.** The Raman spectrum of *h*-BN/SiO_2/Si sample with transfer rate of 95 % shows the fingerprint peak of *h*-BN monolayer at 1368 cm^{-1} at wavelength of 455 nm. The red curves represent the Gaussian fits.

7. Ion conductivity model

The void density of voidal boron nitride (*v*-BN) membranes used in the ion conductivity experiments may be estimated from theoretical considerations. According to the model first proposed by Hall[4] and later adopted by Kowalcyzk et al.[5] and Lee et al.,[6] the conductivity of an ion channel is given by

$$G = \sigma\left(\frac{4L}{\pi D^2}\frac{1}{1+\frac{4l_{Du}}{D}}+\frac{1}{D}\right)^{-1} \quad (1)$$

where σ is the bulk conductivity of the electrolyte, l_{Du} is the Debye length, L is the nominal membrane thickness and D the diameter of an ion channel. The first term in equation (1) is the

transfer conductance, and the second term is the access conductivity G_A. For the given nanopores in a KCl electrolyte with σ= 0.15 S/m that has a Debye length l_{Du} of 3 nm, a nominal membrane thickness L of 1.4 nm and a nanopore diameter D of 2 nm, we get a conductivity of 0.27 nS per nanopore. Thus, we estimate the ”effective” number of voids to be 0, 1.8, 1.3 and 15.9 for the shown 4 membranes in Figure 5F. In comparison, from the nominal void density in the applied v-BN of $2.3\times10^{-3}\mathrm{nm}^{-2}$, an average void number of 4.5 per membrane is expected.

References

1. Corso, M.; Auwärter, W.; Muntwiler, M.; Tamai, A.; Greber, T.; Osterwalder, J. Boron nitride nanomesh. *Science* **2004**, *303*, 217–220.

2. Berner, S.; Corso, M.; Widmer, R.; Groening, O.; Laskowski, R.; Blaha, P.; Schwarz, K.; Goriachko, A.; Over, H.; Gsell, S.; Schreck, M.; Sachdev, H.; Greber, T.; Osterwalder, J. Boron nitride nanomesh: Functionality from a corrugated monolayer. *Angew. Chem. Int. Ed.* **2007**, *46*, 5115–5119.

3. Gorbachev, R. V.; Riaz, I.; Nair, R. R.; Jalil, R.; Britnell, L.; Belle, B. D.; Hill, E. W.; Novoselov, K. S.; Watanabe, K.; Taniguchi, T.; Geim, A. K.; Blake, P. Hunting for monolayer boron nitride: Optical and Raman signatures. *Small* **2011**, *4*, 465–468.

4. Hall, J. E. Access resistance of a small circular pore. *J. Gen. Physiol.* **1975**, *66*, 531–532.

5. Kowalczyk, S. W.; Grosberg, A. Y.; Rabin, Y.; Dekker, C. Modeling the conductance and DNA blockade of solid-state nanopores. *Nanotechnology* **2011**, *22*, 315101.

6. Lee, C.; Joly, L.; Siria, A.; Biance, A.-L.; Fulcrand, R.; Bocquet, L. Large apparent electric size of solid-state nanopores due to spatially extended surface conduction. *Nano Lett.* **2012**, *12*, 4034–4044.